

## High Mobility in LaAlO<sub>3</sub>/SrTiO<sub>3</sub> Heterostructures: Origin, Dimensionality, and Perspectives

G. Herranz,<sup>1,\*</sup> M. Basletić,<sup>1,2</sup> M. Bibes,<sup>3</sup> C. Carrétéro,<sup>1</sup> E. Tafrá,<sup>2</sup> E. Jacquet,<sup>1</sup> K. Bouzouane,<sup>1</sup> C. Deranlot,<sup>1</sup>  
A. Hamzić,<sup>2</sup> J.-M. Broto,<sup>4</sup> A. Barthélémy,<sup>1</sup> and A. Fert<sup>1</sup>

<sup>1</sup>Unité Mixte de Physique CNRS/Thales, Route Départementale 128, 91767 Palaiseau, France

<sup>2</sup>Department of Physics, Faculty of Science, University of Zagreb, Bijenička c. 32–P.O. Box 331, HR-10002 Zagreb, Croatia

<sup>3</sup>Institut d'Electronique Fondamentale, CNRS Université Paris-Sud, 91405 Orsay, France

<sup>4</sup>Laboratoire National des Champs Magnétiques Pulsés, Université Toulouse III, 143 Avenue de Rangueil, 31400 Toulouse, France

(Received 18 January 2007; published 21 May 2007)

We have investigated the dimensionality and origin of the magnetotransport properties of LaAlO<sub>3</sub> films epitaxially grown on TiO<sub>2</sub>-terminated SrTiO<sub>3</sub>(001) substrates. High-mobility conduction is observed at low deposition oxygen pressures ( $P_{O_2} < 10^{-5}$  mbar) and has a three-dimensional character. However, at higher  $P_{O_2}$  the conduction is dramatically suppressed and nonmetallic behavior appears. Experimental data strongly support an interpretation of these properties based on the creation of oxygen vacancies in the SrTiO<sub>3</sub> substrates during the growth of the LaAlO<sub>3</sub> layer. When grown on SrTiO<sub>3</sub> substrates at low  $P_{O_2}$ , other oxides generate the same high mobility as LaAlO<sub>3</sub> films. This opens interesting prospects for all-oxide electronics.

DOI: [10.1103/PhysRevLett.98.216803](https://doi.org/10.1103/PhysRevLett.98.216803)

PACS numbers: 73.40.-c, 66.30.Jt, 73.50.Fq

Among the different technologies that are currently being considered to replace complementary metal-oxide-semiconductor (CMOS) circuits in the coming years, oxide-based electronics is a promising and rapidly growing field [1]. Recently, the interest in the electronic properties of oxide heterointerfaces has been boosted by experiments on LaAlO<sub>3</sub>/SrTiO<sub>3</sub> (LAO/STO) samples, suggesting the existence of a high-mobility conducting layer at the interface between two insulators: a LAO film grown on a STO substrate at pressures smaller than  $10^{-4}$  mbar [2–7].

For such structures, two types of interface can be defined depending on the termination (AO or BO<sub>2</sub>) of the perovskite ABO<sub>3</sub> blocks. The LaO/TiO<sub>2</sub> interface was found to be conductive ( $n$  type) with a large low temperature Hall mobility (up to  $\mu_H \geq 10^4$  cm<sup>2</sup>/V s) and a large sheet resistance ratio [ $R_{\text{sheet}}(300\text{ K})/R_{\text{sheet}}(5\text{ K}) \sim 10^3$ ] [2–6]. On the other hand, the AlO<sub>2</sub>/SrO interface was found insulating. In LAO the La and Al cations have both a 3+ valence, and in STO Sr is 2+ and Ti is 4+. It is argued that the resulting interface electronic discontinuity is avoided through charge transfer from LAO to STO [8]. Within this picture, the high-mobility gas is formed when the LAO layer provides the LaO/TiO<sub>2</sub> interface with half an electron per two-dimensional unit cell, corresponding to  $n_{\text{sheet}} \approx 3.28 \times 10^{14}$  cm<sup>-2</sup>. According to this model, the electronic properties should not depend on the oxygen pressure used to grow the LAO film on the TiO<sub>2</sub>-terminated STO substrate. However, up to now, all the reported high-mobility LAO/STO structures have been grown on STO substrates in reducing conditions ( $P_{O_2} \leq 10^{-4}$  mbar) [2–6].

In parallel, it has recently been demonstrated that the growth of other oxides like Co-doped (La, Sr)TiO<sub>3</sub> (Co-

LSTO) [9] or the homoepitaxial growth of SrTiO<sub>3</sub> films on STO substrates at low pressure ( $P_{O_2} < 10^{-4}$  mbar) [10] also generates a high-mobility conduction, with the same transport properties as the above-discussed LAO/STO structures. However, in those cases charge transfer effects are either different from the LAO/STO case or formally absent. Indeed, the high-mobility conduction in Co-LSTO/STO films has been demonstrated to be due to oxygen vacancy doping of the STO substrates [9]. Therefore, in order to test whether charge transfer across the interface is really responsible for the high-mobility conductive behavior, one should fabricate LAO/STO structures in conditions that prevent the doping of STO substrates by oxygen vacancies, i.e., at pressures well above  $10^{-4}$  mbar [9] and compare these properties with those of structures prepared at smaller pressure.

To address this issue, we have measured the magnetotransport properties of LAO (6–20) nm thick films grown by pulsed laser deposition in a wide range of pressures ( $10^{-6}$ – $10^{-3}$  mbar) on 0.5–1 mm thick TiO<sub>2</sub>-terminated STO(001) single-crystal substrates (for details about magnetotransport experiments see Ref. [9]). The interface was contacted with Al/Au through the LAO layer by locally etching the LAO with accelerated Ar ions down to the interface, in a chamber equipped with a secondary ion mass spectroscopy detection system. The interface has been characterized by aberration-corrected high-resolution transmission electron microscopy (HRTEM), and we have found that the LAO layer is fully strained, and the interface is close to atomically sharp, with no dislocations (the details of HRTEM characterization are reported in Ref. [11]). We note that films cooled down in a high pressure  $P_{O_2} \approx 300$  mbar from the deposition ( $T = 750$  °C) to room temperature were all insulating or highly resistive ( $> 100$  M $\Omega$

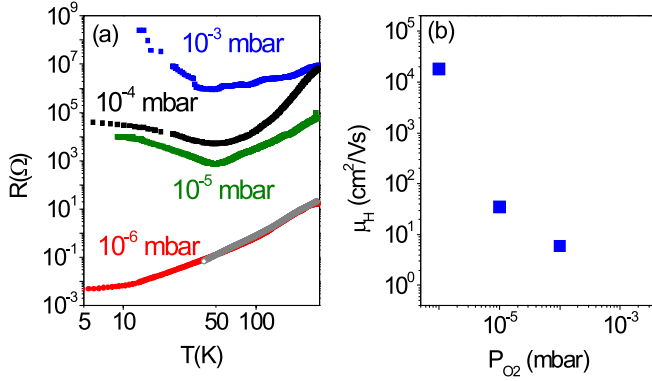


FIG. 1 (color online). (a)  $T$  dependence of the resistance of samples grown at  $P_{O_2} = 10^{-6}$ – $10^{-3}$  mbar; gray symbols correspond to the sample grown at  $10^{-6}$  mbar after removing the LAO film by mechanical polishing (see text) and (b) dependence of the mobility at 4 K ( $\mu_{H,4\text{ K}}$ ) on the deposition pressure.

at room temperature). Consequently, in the following we will report on films cooled down to room temperature in the deposition pressure.

In Fig. 1 we present the dependence on  $P_{O_2}$  of the transport properties of LAO/STO samples with thickness  $t = 20$  nm. The temperature ( $T$ ) dependence of the resistance and mobility of our LAO/STO samples [Fig. 1(a)] grown at low pressure ( $P_{O_2} < 10^{-5}$  mbar) are similar to those reported in other works [2–6]. We observe that the samples become less conductive as  $P_{O_2}$  is higher [Fig. 1(a)]. For films grown at  $P_{O_2} \geq 10^{-5}$  mbar we observe the presence of resistance upturns with nonmetallic behavior below those temperatures. Additionally, the mobility at 4 K ( $\mu_{H,4\text{ K}}$ ) decreases drastically as  $P_{O_2}$  is increased [Fig. 1(b)], and samples grown at  $P_{O_2} \geq 10^{-4}$  mbar show  $\mu_{H,4\text{ K}} < 10$   $\text{cm}^2/\text{Vs}$  (for the sample grown at  $10^{-3}$  mbar the mobility is not measurable). Both observations are at odds with an interpretation based on charge transfer effects.

We proceed now to the analysis of the dimensionality and determination of the thickness of the metallic gas in our LAO/STO sample ( $t = 20$  nm) grown at  $P_{O_2} = 10^{-6}$  mbar. For this sample  $\mu_{H,4\text{ K}} = 1.8 \times 10^4$   $\text{cm}^2/\text{Vs}$  and  $R_{\text{sheet},4\text{ K}} \sim 10^{-2}$   $\Omega/\square$ , in good agreement with data reported in Ref. [2]. Magnetoresistance curves,  $\text{MR} = [R_{xx}(B) - R_{xx}(0)]/R_{xx}(0)$ , were measured with the field  $B$  either perpendicular to the sample plane (PMR), or parallel to the current in the sample plane (LMR). Both magnetoresistances exhibit Shubnikov–de Haas (SdH) oscillations at  $T < 4$  K and magnetic fields  $B \geq 6$  T [the data at 1.5 K are shown in Fig. 2(a)]. Note that these oscillations disappear progressively at  $T > 1.5$  K [see Fig. 2(d)], as expected. After subtracting the background contribution, the SdH oscillations are even more clearly seen in Fig. 2(b). From this figure, it is evident that the period of the oscillations does not depend on the field orientation. The ob-

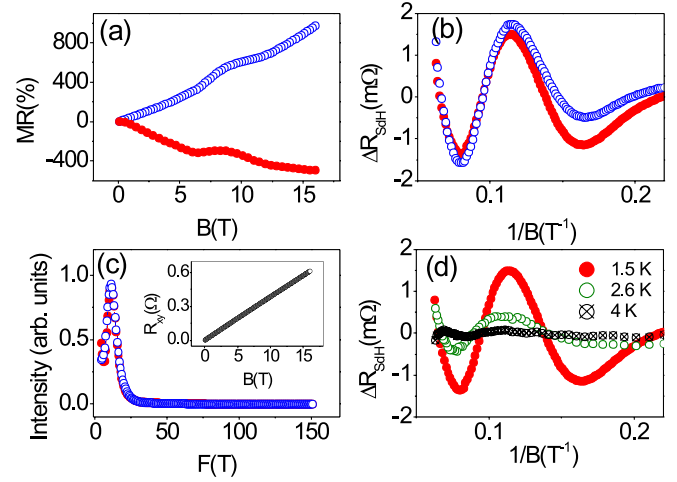


FIG. 2 (color online). (a) Magnetic field dependence of the perpendicular (open symbols) and longitudinal (solid symbols) magnetoresistances at 1.5 K. (b) Oscillatory part of the magnetoresistance  $\Delta R_{\text{SdH}}$ . (c) Spectral power density from FFT analysis of  $\Delta R_{\text{SdH}}(B)$ . (d)  $\Delta R_{\text{SdH}}(B)$  corresponding to perpendicular magnetoresistance at different  $T$ . The inset of (c) shows the field dependence of the Hall resistance  $R_{xy}$  at 4.2 K.

servation of similar SdH oscillations in both configurations excludes any interfacial confinement of carriers.

The SdH oscillations were analyzed following the protocol described in detail in Ref. [9]. The fast Fourier transform (FFT) procedure confirmed that the SdH frequency  $F_{\text{SdH}}$  (which is related to the cross-sectional area  $A_{\text{ext}}$  of extremal electronic orbits in  $k$  space perpendicular to the applied field by  $F_{\text{SdH}} = \hbar A_{\text{ext}}/2\pi e$ ) is the same for the PMR and LMR configurations—cf. Fig. 2(c). This definitely demonstrates that the electronic system is 3D and homogeneous. A system with a nonuniform carrier density (varying as a function of the distance from the film-substrate interface) would lead, in the PMR configuration, to a superposition of different frequencies and to a broadening or blurring of the spectrum.

Furthermore, our data enable us to estimate the thickness of the high-mobility gas. The simplest approximation is to suppose a spherical Fermi surface; in this case, from  $F_{\text{SdH}} \approx 11.1$  T [cf. Fig. 2(c)], we obtain  $k_F \approx 1.8 \times 10^6$   $\text{cm}^{-1}$ . Since the electronic system is 3D, its thickness is thus much larger than the Fermi wavelength  $\lambda_F = 2\pi/k_F \approx 35$  nm. To determine this thickness more precisely, we have used our Hall resistance  $R_{xy}(B)$  data [inset of Fig. 2(c)]. Defining the sheet carrier density  $n_{\text{sheet}}$  as the product of the carrier density  $n$  and the thickness of the metallic region  $t_{\text{hm}}$ , we get  $n_{\text{sheet}} = n \times t_{\text{hm}} = B/(eR_{xy}) \approx 1.6 \times 10^{16}$   $\text{cm}^{-2}$ . The carrier density  $n$  can be determined independently by using the value of  $k_F$  (derived from  $F_{\text{SdH}}$ ); with  $n = k_F^3/3\pi^2 \approx 2 \times 10^{17}$   $\text{cm}^{-3}$ , one finally obtains  $t_{\text{hm}} \approx 800$   $\mu\text{m}$ . Now, if instead of an ideal spherical Fermi surface we use the

more realistic  $k$ -space geometry of doped STO (as described in the Appendix of Ref. [9]), we find  $k_F \approx 0.9 \times 10^6 \text{ cm}^{-1}$ ,  $\lambda_F \approx 70 \text{ nm}$ ,  $n \approx 3 \times 10^{17} \text{ cm}^{-3}$ , and finally  $t_{hm} \approx 530 \mu\text{m}$  which is strikingly close to the substrate thickness. Our analysis unambiguously proves that the high-mobility transport properties of the LAO/STO sample grown at  $P_{O_2} = 10^{-6} \text{ mbar}$  are due to a conducting region homogeneously extending over hundreds of  $\mu\text{m}$  inside the STO substrate. This conclusion is further confirmed by the observation of the same  $T$  dependence [see Fig. 1(a)] of the resistance for a  $10^{-6} \text{ mbar}$  sample before and after removing the film and about  $15 \mu\text{m}$  of the STO substrate by mechanical polishing on the film side [Fig. 1(a)]. This is additional evidence that the transport properties of LAO/STO samples are in fact due to the STO substrate.

For films grown at  $P_{O_2} \geq 10^{-5} \text{ mbar}$ , the sheet resistance increases ( $R_{\text{sheet}} > 1 \text{ k}\Omega$  even at low temperature), and consequently SdH oscillations cannot be observed. However, some insight can be gained by comparing the transport data of LAO/STO structures to those reported for doped bulk STO single crystals. We have collected in Fig. 3 the  $T$  dependence of the mobility [Fig. 3(a)] and normalized resistance [Fig. 3(b)] for STO bulk single crystals (doped or treated in reducing atmospheres) [12], LAO films grown on STO substrates at  $P_{O_2} < 10^{-4} \text{ mbar}$  (this work and Refs. [2,4]), Co-doped (La, Sr)TiO<sub>3</sub> (Co-LSTO) films grown at low  $P_{O_2}$  on STO substrates (Ref. [9]), and STO<sub>3- $\delta$</sub> /STO homoepitaxial films [10]. Let us point out here that one can extract  $\mu_H$  from the Hall experiments without knowing the thickness of the metallic system. This allows a reliable comparison of data from different sources. The main characteristic of both  $T$  dependences [mobility, Fig. 3(a), and normalized resistance, Fig. 3(b)] is the remarkable resemblance of the

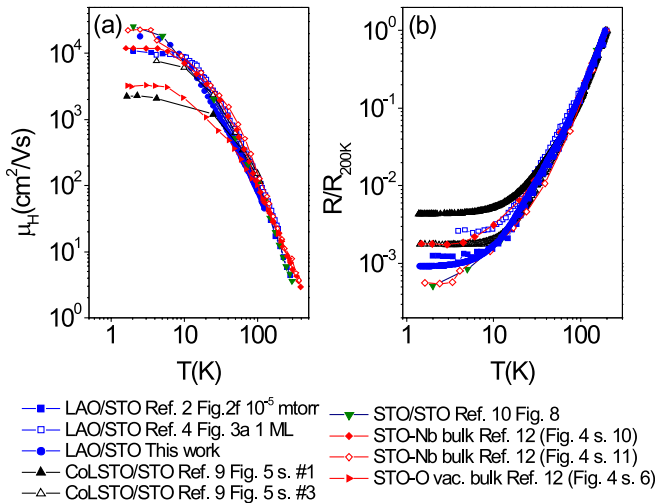


FIG. 3 (color online). (a)  $T$  dependence of the Hall mobility  $\mu_H$  and (b)  $T$  dependence of the resistance normalized to the value at 200 K; both for Co-LSTO/STO, LAO/STO, STO<sub>3- $\delta$</sub> /STO samples, and doped STO single crystals.

behavior for the LAO/STO samples and bulk STO specimens doped with Nb, La, or oxygen vacancies [12–16].

The dependence of the mobility  $\mu_H$  on the carrier density  $n$  for different doped STO single crystals [13,14] is presented in Fig. 4(a). The highest mobilities are observed when the carrier density is  $\sim 3 \times 10^{17} \text{ cm}^{-3}$ . The mobility decays rapidly as  $n$  increases; this is due to the introduction of extrinsic impurities associated to potential fluctuations induced in the lattice. For concentrations below  $10^{17} \text{ cm}^{-3}$ , the impurity band formed by the donors has a reduced width (due to a decrease of the overlap of the impurity wave functions), and the mobility decreases as well. Figure 4(a) also includes our data for Co-LSTO/STO (Ref. [9]) and LAO/STO samples which perfectly match the bulk STO data. The figure is completed by the additional recompilation of the data for STO<sub>3- $\delta$</sub> /STO homoepitaxial films [10] and other LAO/STO samples (Refs. [2,4]), considering that carriers extend over a region of  $500 \mu\text{m}$ . The similarity between the transport properties of LAO/STO samples exhibiting high mobility (grown at  $P_{O_2} < 10^{-4} \text{ mbar}$ ) and those of reduced STO bulk single crystals, suggests that the high mobility of LAO/STO samples might arise from the doping of STO with oxygen vacancies. This conclusion is also supported by recent cathodo- and photoluminescence studies of Kalabukhov *et al.* [17] and by ultraviolet photoelectron spectroscopy of Siemons *et al.* [4].

A remaining question is how far the oxygen vacancies can diffuse into the STO substrates during film deposition. It is known that the exchange of oxygen is strongly enhanced at the film/substrate interface as compared to the

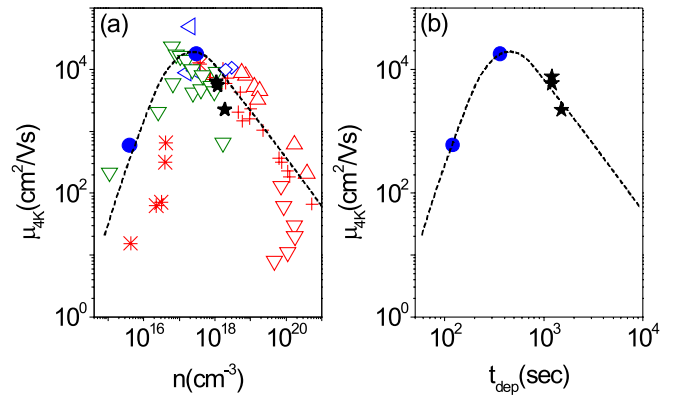


FIG. 4 (color online). (a) Dependence of  $\mu_{H,4K}$  on the carrier density: STO single crystals doped with oxygen vacancies (+) or Nb ( $\Delta$ ) (Ref. [13]); slightly reduced STO single crystals (\*) (Ref. [14]); La-doped STO thin films from ( $\nabla$ ) (Ref. [16]); Co-LSTO/STO samples grown at low pressure (Ref. [9] ( $\star$ )); STO<sub>3- $\delta$</sub> /STO films grown at low pressure ( $\nabla$ ) (Ref. [10]); LAO/STO samples grown at low pressure (Ref. [4]) ( $\diamond$ ), (Ref. [2]) ( $\diamond$ ), and this work ( $\bullet$ ). The dashed lines are guides for the eye. (b) Dependence on time deposition  $t_{\text{dep}}$  of  $\mu_{4K}$  in Co-LSTO (Ref. [9]) and LAO films (this work) grown on STO substrates at low  $P_{O_2}$ .

substrate/vacuum interface [18]. Their diffusion coefficient  $D_V$  has been measured with different methods [19] and at various  $P_{O_2}$  and  $T$ . For  $T \approx 750^\circ\text{C}$  and at pressures as high as  $P_{O_2} \approx 10^{-2}$  mbar, values of  $10^{-4}$ – $10^{-5}$   $\text{cm}^2/\text{s}$  were found. During a time interval  $t$  the vacancies diffuse along a distance  $l_{O\text{ vac}} \approx (D_V t)^{1/2}$ , which is, for  $t = 10$  s (i.e., typical deposition times for the thinnest films) between 100 and 300  $\mu\text{m}$ . It is then reasonable to assume that oxygen vacancies (created when a film is deposited on STO in reducing atmospheres) can extend to a region within the STO substrate compatible with that found from the SdH analysis.

From these considerations, it should be expected that the transport properties are modulated by the effective deposition time  $t_{\text{dep}}$  and, in turn, by film thickness. Figure 4(b) shows the dependence on  $t_{\text{dep}}$  of  $\mu_{H,4\text{ K}}$  when Co-LSTO and LAO films are deposited at  $P_{O_2} \approx 10^{-6}$  mbar on STO substrates. We observe that this  $\mu_{H,4\text{ K}}-t_{\text{dep}}$  curve bears a striking resemblance with the  $\mu_H-n$  curve for the same samples plotted in Fig. 4(a). This is a strong indication that  $t_{\text{dep}}$  increases the density of carriers in the STO substrates. This should also apply at slightly higher pressures  $P_{O_2} \approx 10^{-5}$  mbar, used for growing LAO/STO structures which were reported to have modulated transport properties upon increasing the deposited film thickness [5,6]. Indeed, in an oxygen vacancy-doping scenario, an insulator-metal transition (IMT) should be expected as a function of  $t_{\text{dep}}$  and, therefore, of the number of LAO unit cells grown on the STO substrate [5,6]. When the deposited film thickness increases, the critical concentration  $n_c$  for impurity band formation is reached and an IMT occurs. This behavior is well known in group IV semiconductors doped with impurities [20]. This IMT is accompanied by an abrupt conductivity jump that can be estimated as  $\Delta\sigma_c = n_c \times e \times \mu_c$ , with  $n_c \approx 10^{15}$   $\text{cm}^{-3}$  for doped STO [Fig. 4(a)] and  $\mu_c \approx 1$   $\text{cm}^2/\text{Vs}$  is the mobility at this critical concentration [14]. Substituting values we obtain  $\Delta\sigma_c \approx 1.6 \times 10^{-4}$   $\Omega^{-1}\text{cm}^{-1}$ . If one assumes a conducting thickness  $l \approx 100$   $\mu\text{m}$ , one should observe a conductance jump of  $\Delta G_c \approx \Delta\sigma_c \times l \approx 10^{-5}$   $\Omega^{-1}$  across the IMT. A similar value of  $\Delta G_c$  was reported for the IMT at a critical thickness of LAO films deposited on STO substrates [6].

In summary, we have brought proof of an alternative and coherent explanation for the high mobility in LAO/STO structures based on the doping of STO substrates with oxygen vacancies. This doping is achieved efficiently by the growth of LAO films on STO substrates. This remarkable result might be used to fabricate heterostructures integrating multifunctional oxides with high-mobility STO. For example, spin injection into a STO channel might be achieved with spin-polarized sources such as Co-LSTO [9,21]. Also, an interesting possibility is to dope STO

below the critical concentration  $n_c$ , and to activate the conduction through application of electrical fields. Recent reports on STO channel field-effect transistors with organic [22] or LAO [6] gate insulators evidence enormous field effects in such structures. All these possibilities open interesting prospects and should stimulate further studies of all-oxide structures for spintronics.

G.H. acknowledges financial support from the DURSI (Generalitat de Catalunya, Spain). Financial support from PAI- France-Croatia COGITO Program No. 82/240083 and Croatian MZOS Project No. 119-1191458-1023 is acknowledged. We acknowledge experimental support from Y. Lemaître, S. Fusil, and B. Raquet.

---

\*Electronic address: gervasi.herranz@thalesgroup.com

- [1] S.B. Ogale, *Thin Films and Heterostructures for Oxide Electronics* (Springer Verlag, Berlin, 2005).
- [2] A. Ohtomo and H. Y. Hwang, *Nature (London)* **427**, 423 (2004).
- [3] H. Y. Hwang, A. Ohtomo, N. Nakagawa, D. Muller, and J. Grazul, *Physica (Amsterdam)* **22E**, 712 (2004).
- [4] W. Siemons *et al.*, *Phys. Rev. Lett.* **98**, 196802 (2007).
- [5] M. Huijben *et al.*, *Nat. Mater.* **5**, 556 (2006).
- [6] S. Thiel, G. Hammerl, A. Schmehl, C. W. Schneider, and J. Mannhart, *Science* **313**, 1942 (2006).
- [7] C.W. Schneider, S. Thiel, G. Hammerl, C. Richter, and J. Mannhart, *Appl. Phys. Lett.* **89**, 122101 (2006).
- [8] N. Nakagawa, H. Y. Hwang, and D. A. Muller, *Nat. Mater.* **5**, 204 (2006).
- [9] G. Herranz *et al.*, *Phys. Rev. B* **73**, 064403 (2006).
- [10] A. Ohtomo and H. Hwang, arXiv:cond-mat/0604117.
- [11] J.-L. Maurice *et al.*, *Phys. Status Solidi B* **203**, 2145 (2006).
- [12] O.N. Tufte and P.W. Chapman, *Phys. Rev.* **155**, 796 (1967).
- [13] H. P. R. Frederikse and W. R. Hosler, *Phys. Rev.* **161**, 822 (1967).
- [14] C. Lee, J. Yahia, and J. L. Brebner, *Phys. Rev. B* **3**, 2525 (1971).
- [15] H. P. R. Frederikse, W. R. Thurber, and W. R. Hosler, *Phys. Rev.* **134**, A442 (1964).
- [16] D. Olaya, F. Pan, C. T. Rogers, and J. C. Price, *Appl. Phys. Lett.* **80**, 2928 (2002).
- [17] A. S. Kalabukhov *et al.*, *Phys. Rev. B* **75**, 121404(R) (2007).
- [18] M. Leonhardt, R. D. Souza, J. Claus, and J. Maier, *J. Electrochem. Soc.* **149**, J19 (2002).
- [19] T. Ishigaki, S. Yamauchi, K. Kishio, J. Mizusaki, and K. Fueki, *J. Solid State Chem.* **73**, 179 (1988).
- [20] M. N. Alexander and D. F. Holcomb, *Rev. Mod. Phys.* **40**, 815 (1968).
- [21] G. Herranz *et al.*, *Phys. Rev. Lett.* **96**, 027207 (2006).
- [22] H. Nakamura *et al.*, *Appl. Phys. Lett.* **89**, 133504 (2006).